IC/85/65

INTERNATIONAL CENTRE FOR
THEORETICAL PHYSICS

LIMITING DENSITY RATIOS IN PISTON-DRIVEN COMPRESSIONS

S. Lee

INTERNATIONAL
ATOMIC ENERGY
AGENCY

UNITED NATIONS
EDUCATIONAL,
SCIENTIFIC
AND CULTURAL
ORGANIZATION

1985 MIRAMARE-TRIESTE

International Atomic Energy Agency
and
United Nations Educational Scientific and Cultural Organization
INTERNATIONAL CENTRE FOR THEORETICAL PHYSICS

LIMITING DENSITY RATIOS IN PISTON-DRIVEN COMPRESSIONS *

S. Lee
International Centre for Theoretical Physics, Trieste, Italy,
and
Plasma Research Laboratory, University of Malaya, Kuala Lumpur, Malaysia.

ABSTRACT

By using global energy and pressure balance applied to a shock model it is shown that for a piston-driven fast compression, the maximum compression ratio is not dependent on the absolute magnitude of the piston power, but rather on the power pulse shape. Specific cases are considered and a maximum density compression ratio of 27 is obtained for a square-pulse power compressing a spherical pellet with specific heat ratio of 5/3. Double pulsing enhances the density compression ratio to 1750 in the case of linearly rising compression pulses. Using this method further enhancement by multiple pulsing becomes obvious.

MIRAMARE - TRIESTE
July 1985

* To be submitted for publication.

I. INTRODUCTION

It has been shown [1] from simple energy and pressure considerations that in a fast magnetic pinch-type compression the minimum pinch radius ratio does not depend on the absolute magnitude of the compressing magnetic field power, but only on its time variation. Thus in practical cases the large density compression ratios required to satisfy the concept of a fast pinch reactor [2] cannot be achieved in a single magnetic compression. To enhance the density ratio a current-stepping technique [3] which essentially uses a carefully tailored double compression has been suggested as a possible prelude to further enhancement due to radiation cooling.

For laser driven compressions detailed analysis also indicates that the pellet compression required to achieve appreciable fusion yield in laboratory experiments is not possible with a single spherical shock [4]. This is because of the small size of pellets in a practical controlled experiment. For a solid target pellet of the size say 10 cm in diameter, radiation-driven compression of the solid target pellet to slightly above normal solid density is sufficient. However, even a simple consideration of the scaling of the density containment factor $n\tau$ readily demonstrates that for a controlled fusion solid target, necessarily small, say of the order of 100μ in diameter, a density compression of 10,000-fold solid density is required to fulfill the Lawson criterion. Since it has been demonstrated on the basis of shock computations that a single shock cannot produce the required compression, it has been suggested in the literature [4] that a specified laser pulse be used, so tailored that a sequence of non-overtaking shocks of increasing strength be generated to coalese near the centre of the pellet. After reflection from the centre the coalesced shock will cause a sudden rise in density and temperature sufficient for a successful thermonuclear burn to propagate outwards at supersonic speed. However, it is not clear what laser pulse shape is required to produce the necessary sequence of non-overtaking weak shocks, although specific laser pulse shapes required for isentropic compressions have been discussed [5].

In this paper, the concept of limiting density ratios is re-examined in a simplified general manner without the necessity of going into detailed structure consideration. Using only global energy and pressure consideration, applied to a shock model, limiting compression ratios are obtained for some typical piston power pulse shapes. A double pulse technique is then suggested and the enhanced compression ratios are computed. Using this method, the

[illegible]
limiting values. The required pulse shapes are readily specified and techniques for further enhancement, for example, multiple pulsing, become self-evident.

II. THEORY

1. Shock wave picture

Consider a solid spherical pellet irradiated uniformly by intense radiation as illustrated in Fig.1. The radiation power $R (Js^{-1})$ has associated with it radiation intensity $I = R(4\pi r^2)$ $(Js^{-1}m^{-2})$ and radiation pressure $P_R = I/c = 3.3 \times 10^{-9} R/(4\pi r^2)$ (Nm^{-2}) where c is the speed of light.

Assume that the radiation pressure is fully effective on the surface of the pellet and continues to be fully coupled for the period of the radiation pulse. The radiation pressure will then press on the surface of the pellet like a spherical piston and will maintain this piston-like behaviour as the pellet undergoes compression. This assumption is consistent with the estimation of limiting compression ratios as any deviation from piston behaviour of the radiation-pellet front (for example the pellet surface becoming transparent to the radiation) will result in a lesser value of the gross compression. Assume that the radiation pressure is sufficient to cause the radiation piston to implode supersonically (but non-relativistically). Then a shock front will propagate ahead of the piston; the shock front being the transition region between ambient pellet condition and piston compressed condition. The situation is shown in Fig.2a where both the imploding piston and the converging (forward) shock front are moving inwards.

One property of the shock front converging into the ambient material is that the conservation equations across it require that the shocked plasma behind it be also moving radially inwards. This requires that when the forward spherical shock has converged onto the centre a reflected radially diverging shock front must propagate, behind which the doubly shocked plasma is, on the average across the central sphere, stationary.

One property of the imploding piston is that it is subsonic relative to the plasma heated and compressed by the forward shock driven by the piston. Thus it is a reasonable assumption that the pressure in the region between

[illegible] (labelled region B in Fig.2a) is uniform and is equal to the piston pressure. This is also true of the region between the piston and the reflected shock, also labelled region B in Fig.2b. The reflected shock region (labelled region C in Fig.2b) is a region of both increased density and temperature relative to region B. Hence region C has a higher pressure than region B. We assign a factor f_{rs} to denote the pressure-jump factor across the reflected shock. Thus when the reflected shock hits the radiation piston, the doubly-shocked inner sphere, whose particles have been constrained to be stationary due to the continuous influx of particles from region B, but are now no longer so constrained, disassembles. The situation is as shown in Fig.3. In this figure the point M shows the configuration as the reflected shock hits the radiation piston. It is the point of minimum radius corresponding to maximum compression and the point when according to this model pellet disassembly starts.

2. Energy and pressure equations

Consider the energy in the system at the point of time represented by M. The work done (per unit mass) W by the radiation piston on the target [6] (assuming perfect coupling) in compressing the target from initial radius r_o to radius r is

$$W_m = \frac{1}{(\frac{4}{3}\pi \rho_m r_m^3)} \int_{r_m}^{r_o} \frac{3.3 \times 10^{-9} R(4\pi r^2)dr}{(4\pi r^2)} \qquad (1)$$

where ρ is the mass density, r the piston radius and the subscript m denotes the quantity at the point of time M.

The plasma internal energy U is

$$U_m = \frac{G}{W} X \frac{T_m}{\gamma - 1} \qquad (2)$$

where G is the Universal Gas Constant, W the molecule weight, X the departure coefficient, T the plasma temperature and γ the specific heat ratio.

At the time M, the plasma sphere has no directed kinetic energy, so that, assuming no losses, we may put $W_m = U_m$ and hence obtain the plasma temperature at time M as

$$T_m = \frac{3.3\times 10^{-9}}{\frac{4}{3}\pi \rho_m r_m^3} \frac{(\gamma-1)}{\frac{G}{W}\chi} \int_{r_m}^{r_0} R\,dr \qquad (3)$$

Next we consider the pressure relationship at this time. The plasma kinetic pressure $P_m = (G/W)X\rho_m T_m$ exceeds the radiation pressure P_{Rm} by the reflected shock pressure jump factor f_{rs}. This gives us

$$T_m = \frac{3.3\times 10^{-9}\ R_m f_{rs}}{4\pi r_m^2 \rho_m (G/W)\chi} \qquad (4)$$

From Eqs.(3) and (4) we obtain the combined energy and pressure balance condition as

$$R_m = \frac{3(\gamma-1)}{f_{rs}\, r_m} \int_{r_m}^{r_0} R\,dr \qquad (5)$$

Eq.(5) specifies the radius r_m at which the energy and pressure conditions of Eqs.(3) and (4) are simultaneously met. In order to see the significance of this balance condition we consider here several simple radiation pulses.

Case 1: R = constant. Constant or square pulse radiation power

Take $\gamma = 5/3$, for a fully ionized plasma. With $R = R_m$ = constant, Eq.(5) integrates to

$$k_m = r_m/r_0 = 2/(2+f_{rs}) \qquad (6)$$

and we may construct a table to give us the radius ratio and density ratio $\rho_m/\rho_0 = k_m^{-3}$ at maximum compression as a function of the reflected shock pressure ratio f_{rs} taken as a parameter from 1 to 10.

f_{rs}	k_m	ρ_m/ρ_0
1	0.67	3.38
1.5	0.57	5.36
2	0.5	8
3	0.4	15.6
4	0.33	27.
5	0.29	42.9
6	0.25	64
10	0.17	216

It is instructive to follow values of the LHS function F_L and RHS function F_R of Eq.(5) as the compression proceeds from k = 1. This is normally computed during a trajectory computation, but in this case since this problem is being solved without a trajectory computation we indicate these function values schematically in Fig.4 for the three cases $f_{rs} = 1$, $f_{rs} = 4$ and $f_{rs} = 10$. In this figure the points M_1, M_2 and M_3 represent the intersection points of the curves F_R and F_L, respectively, for the cases of $f_{rs} = 1$, $f_{rs} = 4$ and $f_{rs} = 10$. These points represent the points of maximum compression, respectively for the three cases as expressed by Eq.(5).

It is seen that for a given pulse shape of R the compression depends strongly on the value of f_{rs}. von Guderley [7] has shown that the value of f_{rs} near the point of reflection is typically about 6, 4.5 and 3.5, respectively, for planar, cylindrical and spherical shocks. We shall take the value of $f_{rs} = 4$ for our consideration. Using this value of f_{rs} for the case of square pulse radiation power, the radius ratio k_m is 0.33 corresponding to a density ratio of 27.

Case 2: $R = R_m(r-r_0)/(r_m-r_0)$. Radiation power linearly rising with decreasing r

For this case Eq.(5) integrates to

$$k_m^2 - k_m = \frac{3}{f_{rs}}(\gamma-1)(k_m - k_m^2/2 - 1/2) \qquad (7)$$

which for $\gamma = 5/3$ and $f_{rs} = 4$ gives

$$k_m = 0.2 \quad \text{and} \quad \rho_m/\rho_0 = 125 \ .$$

Thus a rising radiation power during compression gives rise to greater compression than a constant power. This is evident from an analysis of Eq.(5) or the schematic of Fig.4. It is also evident from Eq.(5) that a pulse which rises faster than that of Case 2 will produce even greater compression.

Case 3: Double pulse. Both pulses of constant power; the second pulse has n times the amplitude of the first pulse

The advantage of using a double pulse may be seen from Eq.(5). Let us follow the functions F_R and F_L of Eq.(5) during a compression using constant power. From Fig.4 we have seen that for $f_{rs} = 4$ the values of F_R and F_L converge at k = 0.33. If as this point is approached, the radiation power is stepped up to n times the amplitude of the first pulse then the convergence point of F_R and F_L is shifted to a smaller value of k as shown in Fig.5 where it is seen that a new balance point $k_m < 0.33$ is established.

In practice because the reflected shock will have hit the piston despite the sudden rise of piston power to nR_m, it is necessary for the value of n to be greater than f_{rs}. We take the case of $n = 6$ and assume that when the piston reaches $k = k_1$ where $k_1 \gtrsim 0.33$ the radiation power is stepped up to $6\,R_m$. Then when the reflected shock hits the piston, the reflected shock is turned back towards the axis, reflects off the axis and again moves towards the piston, hitting it with a pressure rise factor again of four times the increased piston pressure of $6\,R_m$. Then a re-examination of Eqs.(1)-(4) for this situation shows that Eq.(5) now becomes

$$nR_m = \frac{3(\gamma-1)}{f_{rs}\, r_m} \left(\int_{r_1}^{r_0} R_m\, dr + \int_{r_m}^{r_1} n R_m\, dr \right) \tag{8}$$

giving for $\gamma = 5.3$, $f_{rs} = 4$, $n = 6$ and $k_1 = 0.4$:

$$12\, k_m = \int_{0.4}^{1} dk + 6\int_{k_m}^{0.4} dk \tag{9}$$

so that we have $k_m = 0.17$ and $\rho_m/\rho_0 = 204$. Thus this double pulse technique has increased the density compression 7-fold as compared with a single pulse.

Case 4: Double pulse. Both pulses linearly rising with decreasing r, the second pulse with a gradient $n = 6$ times that of the first pulse

In this case, switching the second pulse on when the piston has reached $k = 0.3$ (noting from Case 2 that the balance point for the first pulse only is at $k = 0.2$) gives $k_m = 0.083$ with corresponding density ratio of 1750; a 14-fold increase in density compression when compared to the single linear pulse.

III. DISCUSSION

The above cases have been chosen for simplicity of interpretation and of integration of Eq.(5) without the need to obtain the trajectory. In an experimental situation the power pulse would be specified as a function

of time, rather than of radius, so that the computation of F_R of Eq.(5) would have to be done simultaneously with the computation of the trajectory $r(t)$ as a function of time. For simplicity we may use a snowplow model such as

$$\frac{d}{dt}\left((r_0^3 - r^3)\frac{dr}{dt} \right) = - \frac{3.3 \times 10^{-9}}{\frac{4}{3}\pi \rho_0} R(t) \tag{10}$$

This equation normalizes to

$$\frac{d}{d\tau}\left((1-k^3)\frac{dk}{d\tau} \right) = -\alpha^2 \mathcal{R} \tag{11}$$

where $k = r/r_0$, $\tau = t/t_0$, $\mathcal{R} = R/R_0$, with scaling parameter $\alpha = t_0/t_p$, where t_0 would be associated with a characteristic time (for example rise time) of the radiation pulse and t_p is given by

$$t_p = \left(\frac{4\pi \times 10^8 \rho_0 r_0^4}{R_0} \right)^{1/2} \tag{12}$$

For example taking $\alpha = 1$, $r_0 = 10^{-4}$ m, $\rho_0 = 10^3$ kg m^{-3} then we have

$$t_p = t_0 = 10^{-2} R_0^{-1/2} \tag{13}$$

where t_p may be interpreted as the characteristic time of the compression. Some characteristic times and speeds are deduced from Eq.(13) as follows:

R_0 (pulse peak power)	t_p (characteristic compression time)	r_0/t_p (characteristic compression speed)
(Watt)	(ns)	(ms^{-1})
10^{13}	3	3×10^4
10^{14}	1	10^5
10^{15}	0.3	3×10^5
10^{16}	0.1	10^6

For a given radiation pulse $R(t)$, Eq.(11) may be solved for selected values of α. This equation by itself gives a trajectory which goes to $r = 0$, a non-physical situation. However, with the concurrent use of Eq.(5), the limit of the trajectory may be determined. A more realistic model such as the slug model may, of course, also be used.

IV. CONCLUSION

The limits of compression for magnetic drivers as well as radiation drivers are determined by energy and pressure considerations. The specific case of a radiation driven pellet compression is considered here. The radiation pulse is considered to interact with the pellet as a piston driving a strong shock which upon convergence at the centre reflects towards the piston with a pressure rise factor of 4. Using this model an energy-pressure balance condition is derived for the radius of maximum compression. The physics of this balance condition is then demonstrated by considering several simple cases. These are summarized here:

	minimum radius ratio	maximum density compression
R = constant; square pulse radiation power	0.33	27
$R = R_m \frac{(r-r_0)}{r-r_m}$; power linearly rising	0.2	125
Double pulse; both constant power, n = 6	0.17	204
Double pulse; both with linearly rising power, n = 6	0.083	1750

The method is simple and gives new insight into the limits of compression as simply a condition set by energy and pressure balance. The method also gives an indication as to how these limits may be extended by pulse shaping. It is applicable to pulse shapes of any type. Since the method assumes no losses and perfect piston coupling, any losses or imperfection in coupling would give lower compression ratios than those indicated. Thus the method gives the gross maximum compression for each pulse shape. The method may easily be extended to multiple pulse steps of number greater than 2, with consequent greater compressions.

ACKNOWLEDGMENTS

The author would like to thank Professor Abdus Salam, the International Atomic Energy Agency and UNESCO for hospitality at the International Centre for Theoretical Physics, Trieste, where this work was completed. The research grant F95/77 of the University of Malaya is also acknowledged.

REFERENCES

[1] S. Lee, Bul. Fiz. Malaysia 2, 240 (1981); Plasma Phys. 25, 571 (1983).

[2] M.G. Haines, Phys. Scr. T2/2, 380 (1982).

[3] S. Lee, J. Phys. D 17, 733 (1984).

[4] S.V. Lawande, M.R. Gunye and S.V.G. Menon, Pramana 14, 271 (1980).

[5] R.E. Kidder, Nucl. Fus. 14, 797 (1974).

[6] S. Lee, J. Fiz. Malaysia 5, 53 (1984).

[7] G. von Guderley, Luftfahrtforschung 19, 302 (1942).

FIGURE CAPTIONS

Fig.1 Idealized representation of spherical compression of pellet by radiation piston.

Fig.2 a) Imploding radiation piston driving a converging (forward) shock, before the forward shock has hit the centre. Region A = ambient pellet condition, region B = piston compressed (singly shocked) condition.

b) Imploding radiation piston driving a diverging (reflected) shock, after the forward shock has hit the centre. Region B = singly shocked region, region C = doubly shocked region.

Fig.3 Trajectory of pellet compression showing regions A, B and C of Fig.2.

Fig.4 Illustrating the convergence of function values F_L and F_R of Eq.(5) for a square pulse.

Fig.5 Illustrating the effect of a stepped square pulse in shifting the convergence point of functions F_L and F_R to a smaller radius.

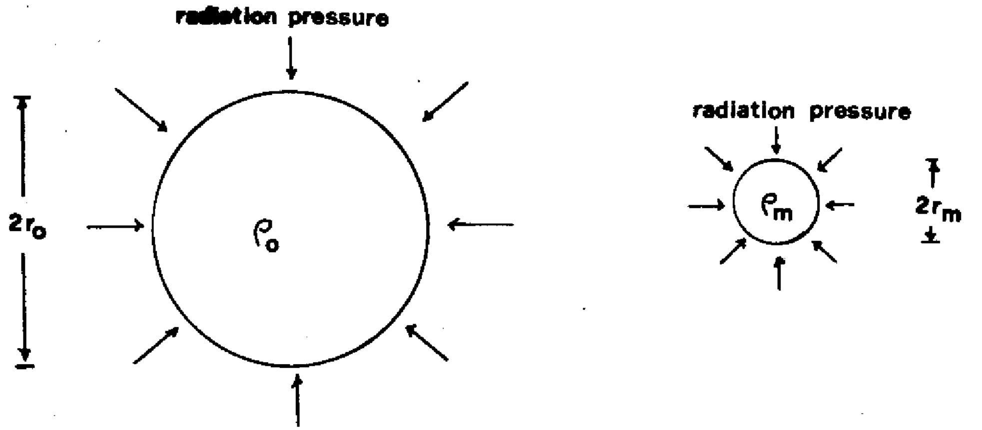

(a) initial geometry

(b) maximum compression geometry before disassembly

Fig.1

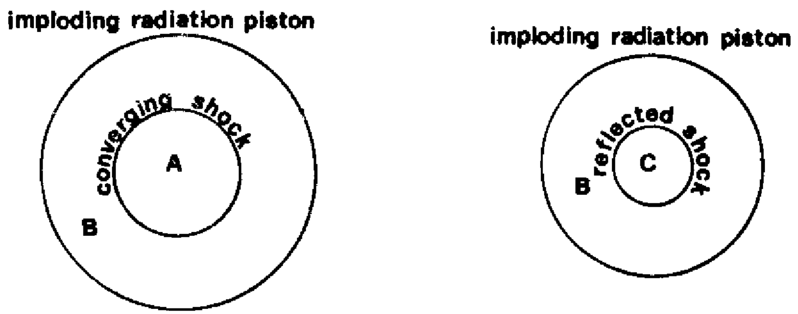

(a)

(b)

Fig.2

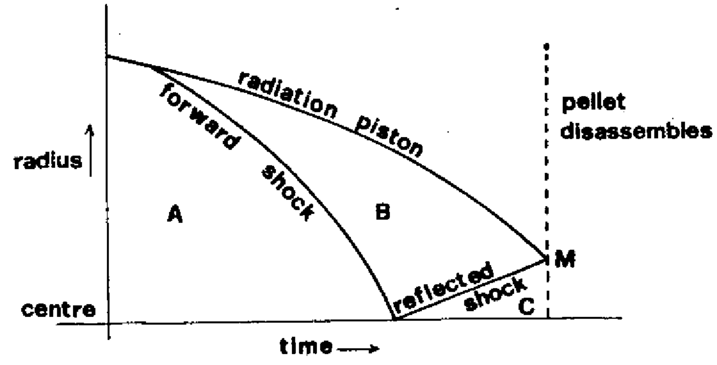

Fig.3

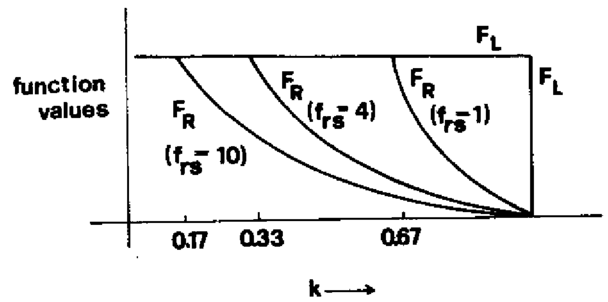

Fig.4

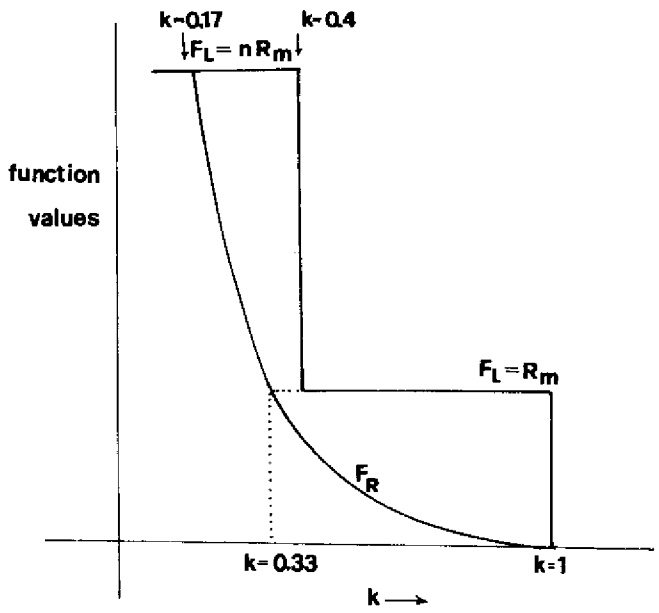

Fig.5